J Mol Model (2011) 17:3275–3288
DOI 10.1007/s00894-011-1004-9

ORIGINAL PAPER

# Complexation of alkali metal cations by crown-ether type podands with applications in solvent extraction: insights from quantum chemical calculations

**Mário Valente · Sérgio Filipe Sousa · Alexandre L. Magalhães · Cristina Freire**

Received: 1 December 2010 / Accepted: 31 January 2011 / Published online: 4 March 2011


**Abstract** The complexation behavior of nine polyether type podands with a varying number of oxygen donor atoms (4–10) towards the alkali metal cations $Li^+$, $Na^+$ and $K^+$ was studied by quantum chemical methods at the DFT-B3LYP level of theory using the all-electron split-valence 6-311++G(d,p) basis set. The optimized structures of the complexes show a regular increase in the mean cation–oxygen distance with the coordination number. OC–CO dihedral angles of the podand arms were also found to increase with the coordination number and with the size of the cation. Maximum values for the number of strong cation–oxygen interactions (effective coordination numbers) were found for each cation (six for $Li^+$, seven for $Na^+$ and eight for $K^+$). The calculated values for thermodynamic parameters relative to the binding of free and solvated cations to the podands allowed the assessment of binding constants in vacuum, in water and in dichloromethane. The estimated cation extraction constants mimic the experimental extraction trends, but their values are much larger than experimental values. Scale factors were determined to correct the values effectively. For each podand the ratios between the calculated extraction constants of $Li^+$ (or $Na^+$) and the corresponding ones for $K^+$ (seen as extraction selectivities) compare acceptably with the corresponding experimental values.

**Keywords** Podands · Alkali metal cation extraction · DFT theory

**Electronic supplementary material** The online version of this article (doi:10.1007/s00894-011-1004-9) contains supplementary material, which is available to authorized users.

M. Valente · S. F. Sousa · A. L. Magalhães (✉) · C. Freire
Departamento de Química e Bioquímica,
Faculdade de Ciências da Universidade do Porto, Requimte,
Rua do Campo Alegre,
4169-007 Porto, Portugal
e-mail: almagalh@fc.up.pt

C. Freire
e-mail: acfreire@fc.up.pt

## Introduction

The discovery of the complexation of alkali metal cations with crown ethers (coronands) by Pedersen [1, 2] inspired many workers to study the complexation behavior of polyethers towards alkali and alkaline earth ions. As coronands were considered good models for naturally occurring ionophores [2–4], they stimulated considerable interest among theoretical chemists. Early theoretical work on the complexation of alkali metal cation complexes by crown ethers was done using molecular mechanics (MM) and molecular dynamics (MD) techniques [5, 6] as they are much less demanding of computer time than quantum calculations because of the (typically large) number of atoms involved, in particular when explicit solvents are involved. In fact, most of the theoretical work on polyether systems has been done at the MM/MD level and specifically on cyclic (coronands) [5–17] or polycyclic polyethers (criptands) [11, 18–20]; linear polyethers (podands) have been addressed only marginally [21, 22] despite the increasing interest they attract as phase transfer catalysts [23–29] and extraction agents [21, 22, 30–37].

It is pertinent to present here a small review of the theoretical work done at the quantum level involving coronands (in view of the absence of such studies with podands) as both systems share strong structural similarities.

In two early works, Yamabe et al. studied the complexation of 12-crown-4 and 18-crown-6 with alkali metal cations,

using the CNDO/2 [38] and ab initio methods [39] with a minimal basis set. These authors reported the importance of considering the solvation of both the cation and the complex in order to achieve acceptable energetic predictions for the complexation step. They found that the size fit between the crown ether hole and the cation diameter does not always define crown ether selectivity, and that the electrostatic interaction between the crown ether donor atom lone pairs and the cation is not necessarily the dominant factor in stabilization of the complex as charge transfer also contributes to it.

Ha and Chakraborty [40] were the first to apply the Kohn-Sham density functional theory (DFT), with a local density approximation (LDA) functional, to the 18-crown-6 molecule and its ammonium complex, aiming to achieve potential energy functions for use in Monte-Carlo simulations.

Glendening et al. [41] performed calculations at the RHF level using 3-21 G and 6-31 G(d) basis sets and relativistic electron core potentials (ECP) on complexes of 18-crown-6 with the alkali metal cations ($Li^+$ to $Cs^+$). The affinity of the coronand towards the cations was estimated to vary between 50 and 100 kcal $mol^{-1}$ and the ligand-to-cation charge transfer interaction was considered to be less important (20–50%) than the electrostatic interaction. The experimental selectivity sequence found in water for this crown ether was recovered only when four waters of hydration were considered.

Feller [42] studied the effect of microsolvation (considering up to nine solvation water molecules) on the binding affinities of 18-crown-6 for the alkali metal cations ($Li^+$ to $Cs^+$). In his work, he used second order Møller-Plesset (MP2) perturbation theory with full Boys-Bernardi counterpoise (CP) corrections and a 6-31+G(d) basis set altered for the heavier elements ($K^+$ to $Cs^+$) with ECPs to estimate the binding energy of Hartree Fock (HF) 6-31+G* optimized structures. The hydration of the cation in the exchange reaction

$$K^+(H_2O)_n + [M(18-crown-6)]^+ \rightleftharpoons [K(18-crown-6)]^+ + M^+(H_2O)_n \quad (1)$$

(with *n* higher than 3) should be taken into account in order to recover the experimental selectivity sequence in water and to achieve qualitative agreement between the experimental and calculated binding enthalpies. In another comparative study on the different selectivities shown by 18-crown-6 and a structurally more rigid but similar ionophore, Feller et al. [43] used the same computational protocol as before and recognized once again the importance of considering the cation hydration with up to four water molecules in the above mentioned exchange reaction to achieve at least qualitative agreement with experimental data as far as selectivity is concerned.

Hill et al. [44] used RHF and MP2 levels of theory with various basis sets (from 6-31+G(d) up to aug-cc-pVTZ) to study the interaction between alkali metal cations and 1,2-dimethoxyethane or 12-crown-4, and found a marked dependence of the OC–CO dihedral angle (in particular for the open chain molecule) and of the $M^+$–O distance on the size of the cation. The comparison of experimental and calculated dissociation enthalpies was considered generally good but some considerable discrepancies (up to 14 kcal $mol^{-1}$) occurred. These were tentatively attributed to neglected high energy conformers.

More recently, Ali et al. [45] reported high level calculations performed using the DFT B3LYP level of theory and the 6-311++G(d,p) basis set on a series of coronands (from dioxane to 18-crown-6) and their $Li^+$ and $Na^+$ complexes. These authors reported structural and energetic features for the free coronands and the complexes, and attempted binding energy calculations considering gas phase reactions between the cations and the free podands. The binding was found to be stronger for the $Li^+$ complexes than for the $Na^+$ ones, and it increased with the number of donor oxygen atoms present in the coronand.

Diao et al. [46] performed calculations at the B3LYP/6-31 G(d,p) level of theory on alkali ($Li^+$, $Na^+$ and $K^+$) complexes with 12-crown-4. These authors estimated the cation extraction distribution constant by considering it equivalent to the quotient between the (in vacuum) complex formation constant and the tetrahydrated cation formation constant.

Hou et al. [47] performed calculations at the B3LYP/6-31 G(d) level of theory on several coronands, all with four oxygen atoms but different sizes (12–16 atoms), and their $Li^+$ and $Na^+$ complexes. They concluded that, under vacuum, $Li^+$ cation invariably form the most stable complexes, independently of ring size.

De et al. [48] used the 6-311++G(d,p) basis set at the B3LYP level of theory to perform energy calculations on optimized structures (at the MP3 level of theory) of complexes involving $Li^+$ and $Na^+$, and several simple coronands, with a varying number (1–7) of potential donor oxygen atoms. They found that the cation-to-coronand binding energy increased with the increase in the number of oxygen atoms until a number of six was present (18-crown-6). For the coronand with seven oxygens (21-crown-7) the binding energy was actually found to decrease. These authors reported that, under vacuum, the binding energy and selectivity towards $Li^+$ is always higher than towards $Na^+$ but the effect of micro-solvation of the cations by six molecules of water inverts this tendency.

The present work stems from our ongoing investigation into the complexation and extraction capabilities of polyether type podands towards alkali metal cations. To the best of our knowledge, it constitutes the first work to address

this subject at the quantum chemical level in a systematic way.

## Computational protocol

The systems studied in the present work—polyether podands (Fig. 1 [1]) and their alkali metal ($Li^+$, $Na^+$ and $K^+$) cation complexes—are quite demanding as far as quantum chemical methods are concerned. Even the smallest systems (b11 and b02) comprise a relatively large number of atoms, thus requiring a considerable number of basis functions at even modest levels of theory. These systems show very flexible structures and the search of minima in the conformational phase-space is near to impossible. Nonetheless, stable structures (local minima) for these systems are very close in terms of energy as hinted at by a unpublished study performed at the HF/6-31 G(d) level of theory on 22 different conformations of the isolated b33 molecule, for which the mean free energy of formation is 2.42±2.14 kcal $mol^{-1}$ and the mean formation enthalpy is 1.75±1.11 kcal $mol^{-1}$, both relative to the values found for the most stable conformation ($g^+g^+g^+g^+g^+g^+$). As starting structures, we chose $g^+g^-$ alternating conformations for the OC–CO dihedral angles of the podand arms as these conformation sets allow the podands to achieve coordination prone structures and may be considered as acceptable representative structures for the systems under study.

DFT was chosen as the fundamental level of theory in our work as it has been used widely to study similar systems (e.g., coronands, see above) and is considered to be an adequate method to predict structural and thermodynamical properties [49]. Among the various DFT functionals, we chose the hybrid B3LYP [49, 50] as it is nowadays widely tested and used.

Optimization and energetic analysis of the free podands and their alkali metal cation complexes was carried out with the GAUSSIAN 03 package [51] using the all-electron 6-311++G(d,p) basis set. All geometry optimizations were performed using the "tight" gradient conversion threshold of GAUSSIAN03. The resulting structures were used for hessian calculations in order to analyze their stationary nature (by looking for the number of imaginary vibrational frequencies) and to estimate corresponding zero-point corrected enthalpies ($H$) and free energies ($G$) of formation at 298 K [52].

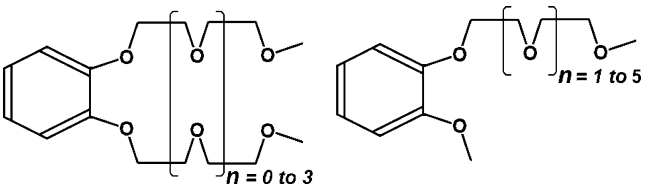


**Fig. 1** Schematic representation of the symmetric (*left*) (b11–b44) and asymmetric (*right*) (b02–b06) podands studied in the present work

Optimized structures of the tetrahydrated cations were considered with the water molecules in a tetrahedral arrangement (with the dipoles pointing towards the alkali cations) because this structure is known to constitute the lowest energy one for this hydration number and has been used in similar studies before [53, 54]. No studies were found in the literature on alkali cation solvation in dichloromethane, thus we performed a series of calculations involving two to four solvent molecules. The corresponding optimized geometries consisted of a linear arrangement, a triangular arrangement and a tetrahedral arrangement for the dichloromethane molecules surrounding each of the cations, considering in all cases the global solvent dipole directed towards the cation (at this point we must stress that these are merely "guess structures"). In the subsequent thermodynamical calculations we considered the dichloromethane tetra-solvated cations, as these were found to be the lowest energy cations (higher solvation numbers than four and other solvation geometries were not tried for steric reasons).

The full Boys and Bernardi [55] counterpoise correction was also applied to the calculation of the interaction energies reported, to account for the basis set superposition error (BSSE).

## Results and discussion

The optimized structures found for the free podands, for the complexes and for the solvated cations correspond to local minima of the potential energy surface as confirmed by the absence of imaginary frequencies of molecular vibration.

The optimized structures of the complexes are presented in Fig. 2 and structural data relevant for the following discussion are compiled in Tables S1–2 in the electronic supplementary material. For each complex, the mean cation-to-podand oxygen distances and OC–CO dihedral angles are presented in two columns: in the first, the mean values are presented considering the total number of oxygen atoms present in the podand ($d_{total}$, $\varphi_{total}$), and in

[1] The symbology used in the present work to designate the podands is based on the number of ethylene glycol (eg) units present in each of the two arms, always bonded to the aromatic ring at ortho positions. So, podand b33 has two equal sized arms consisting of chains with three eg units, comprising a total of eight potentially donor oxygen atoms, bonded at ortho positions to the aromatic ring, and podand b06 has one arm consisting of a chain with six eg units and one methoxy group, comprising a total of eight potentially donor oxygen atoms, bonded at ortho positions to the aromatic ring. Thus, to find the number of potentially donor oxygen atoms of podand b"mn" one just has to perform the sum: m+n + 2.

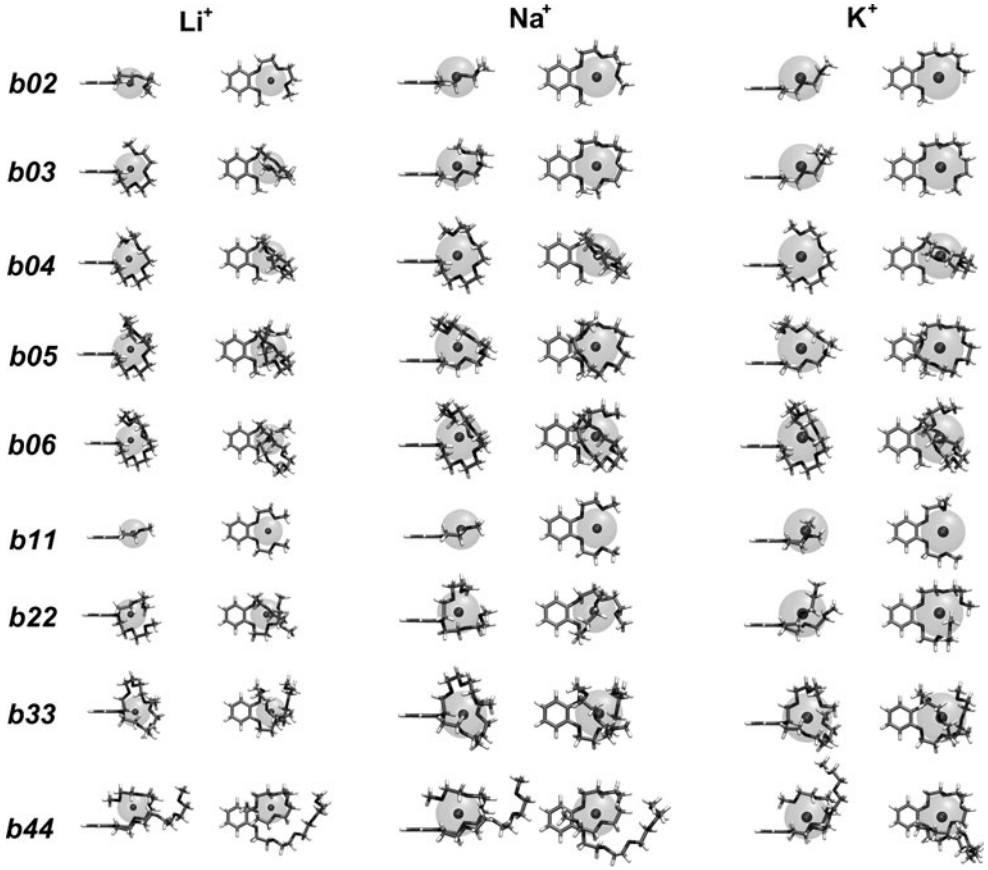


**Fig. 2** Optimized structures for the complexes of $Li^+$, $Na^+$ and $K^+$ with the podands b02–b06 and b11–b44, each in parallel (*left*) and perpendicular (*right*) view (relative to the aromatic ring)

the second, only those oxygen atoms involved in strong interactions with the cation were considered ($d_{partial}$, $\varphi_{partial}$). Throughout the present work, we consider the interaction between the cation and a podand oxygen to be strong when its inter-atomic distance is not greater than 20% of the mean $M^+$–O distance found for that complex (naturally, in the calculation of these mean distances we did not consider completely unbound oxygen atoms).

## Structural features of the optimized complexes

In this section we present a comparative characterization of the structural features found for the optimized complex structures involving the cations $Li^+$, $Na^+$ and $K^+$ and each of the podands (b02–b06 and b11–b44).

### *Complexes with $Li^+$*

All the oxygen atoms of the b11 and b02 podands participate in strong interactions with the $Li^+$ cation and the mean $Li^+$–O distances found are 2.013 Å (±0.003) and 1.986 Å (±0.008), respectively. The mean OC–CO dihedral angles determined are, respectively 47.9° (±0.1) and 50.8° (±0.5), with distorted square planar complex geometries. For the complex with b03, all five podand oxygen atoms participate in strong interactions with the cation, showing a mean $Li^+$–O distance of 2.050 (±0.040) Å, a mean OC–CO dihedral angle of 52.7° (±1.1) and a near square pyramidal geometry. The complexes of $Li^+$ with the podands b22 and b04 show different coordination numbers (5 and 6, respectively) as in the symmetrical podand one of the oxygen atoms is at 3.018 Å from the cation. The six strongly interacting oxygen atoms of b04 in the complex are at a mean distance of 2.257 (±0.146) Å, the five strongly interacting oxygen atoms of b22 are at a mean distance of 2.103 (±0.056) Å, and the corresponding geometries are octahedral and pentagonal pyramidal, with mean OC–CO dihedral angles of 52.8° (±2.7) and 52.6° (±1.5), respectively. The potentially heptacoordinating b05 podand established only six strong interactions with the $Li^+$ cation, with a mean distance of 2.262 (±0.146) Å; the seventh oxygen atom is at 2.943 Å from the cation. The coordination geometry is of the distorted octahedral type, with a mean OC–CO dihedral angle of 54.8° (±1.1). The b33 and b06 podands are potentially octacoordinating but in both cases they show pentacoordination with $Li^+$. Here, the mean $Li^+$–O distances are 2.216 (±0.042) Å and 2.114 (±0.078) Å, respectively, with the extra oxygen atoms at 3.555 Å, 3.690 Å and 3.833 Å for the first podand and 3.151 Å, 3.995 Å and 4.075 Å for the second podand. The corresponding coordination geometries are both of the distorted pentagonal pyramidal type, with OC–CO dihedral

angle values of 50.5° and 52.2° (±4.0), respectively. As for the *b44* podand, with ten potentially donor oxygen atoms, the $Li^+$ complex is pentacoordinated to the oxygen atoms of only one of the arms, at a mean distance of 2.134 (±0.087) Å, forming a pentagonal pyramidal complex geometry with a mean OC–CO dihedral angle value of 52.4° (±4.0). The other oxygen atoms are at 3.399 Å, 4.769 Å, 6.046 Å and 6.256 Å from the cation.

On the whole, the $Li^+$–O mean distance increases steadily with the increase of the coordination number: 2.000 (±0.019) Å for the tetracoordinated cation (considering the complexes involving podands b02 and b11), 2.090 (±0.039) Å for the pentacoordinated cation (considering the complexes involving podands b03, b06, b22, b33 and b44) and 2.260 (±0.003) Å for the hexacoordinated cation (considering the complexes involving podands b04 and b05). The mean OC–CO dihedral angle is also found to increase from 49.4° (±2.1°) in the case of tetracoordination to 52.5° (±1.3°) in the case of pentacoordination, and further to 53.7° (±1.6°) in the case of heptacoordination.

*Complexes with $Na^+$*

In the optimized structures of the $Na^+$ complexes with b11 and b02, all four oxygen atoms interact strongly with the cation and the $Na^+$–O mean distances are 2.325 (±0.003) Å and 2.325 (±0.007) Å, respectively. The corresponding complexation geometries are both distorted square planar with mean OC–CO dihedral angles of 54.2° (±0.1°) and 55.5° (±2.4°), respectively. The complex with b03 shows a nearly pentagonal planar geometry with a mean $Na^+$–O distance of 2.397 (±0.037) Å, and a mean OC–CO dihedral angle value of 56.0° (±1.9°). With the b22 and b04 podands, all oxygen atoms interact strongly, with mean $Na^+$–O distances of 2.430 (±0.032) Å and 2.438 (±0.031) Å, respectively. The geometries found were distorted octahedral and pentagonal pyramidal, and the corresponding mean dihedral angle values are 57.6° (±1.5°) and 58.1° (±1.7°), respectively. All seven oxygen atoms of the b05 podand interact strongly with the cation at a mean distance of 2.558 (±0.086) Å and a mean OC–CO dihedral angle value of 57.4° (±1.4°). The complexes of $Na^+$ with both potentially octadentate podands b33 and b06 do not involve all oxygen atoms in complexation: the first forms a hexacoordinate complex with a mean $Na^+$–O distance of 2.542 (±0.079) Å, and the second forms a heptacoordinate complex with a mean $Na^+$–O distance of 2.621 (±0.098) Å. The other, non strongly interacting, oxygen atoms are at 3.171 Å and 3.526 Å from the cation, for the *b33* complex, and 2.983 Å from the cation, for the b06 complex. The mean dihedral angle values are 58.2° (±4.8°) and 61.2° (±1.2°), respectively. The structure of the complex formed between the cation and the potentially decadentate *b44* podand shows hexacoordination, with a mean $Na^+$–O distance of 2.567 (±0.065) Å, and a mean OC–CO dihedral angle value of 57.8° (±1.3°). The other oxygen atoms are at 3.931 Å, 4.762 Å, 6.163 Å and 6.681 Å from the cation.

The $Na^+$–O mean distance was found to increase from 2.325 (±0.001) Å in the tetracoordinated cation (considering complexes involving podands b02 and b11) to 2.397 Å for the pentacoordinated cation (considering the complex involving podand b03), to 2.475 (±0.052) Å for the hexacoordinated cation (considering complexes involving podands b04, b22, b33 and b44) and to 2.590 (±0.044) Å for the heptacoordinated cation (considering complexes involving podands b05 and b06). The mean OC–CO dihedral angle also increases from 54.8° (±0.9°) in tetracoordination to 56.0° in pentacoordination, to 57.9° (±0.2°) in hexacoordination, to 59.3° (±2.7°) in heptacoordination.

*Complexes with $K^+$*

The optimized structures for the complexes of $K^+$ with the podands b11 and b02 showed that all podand oxygen atoms participate in strong interactions with the cation, with a mean $K^+$–O distance of 2.718 (±0.008) Å and 2.714 (±0.019) Å, respectively. The resulting coordination geometries are strongly distorted square planar due to the size of the cation, and the corresponding mean dihedral angle values are 60.4° (±1.5°) and 60.5° (±1.1°). In the complex with podand b03, the five oxygen atoms also establish strong interactions with the cation, with a mean distance of 2.756 (±0.013) Å and a planar distorted pentagonal geometry with a mean dihedral angle value of 61.9° (±1.4°). The complexes of $K^+$ with the podands b22 and b04 also involve all oxygen atoms and the mean $K^+$–O distances are 2.840 (±0.047) Å and 2.787 (±0.024) Å, respectively, and the corresponding geometries found are distorted hexagonal and nearly pentagonal pyramidal with mean dihedral angle values of 61.5° (±0.2°) and 63.1° (±0.8°), respectively. The complex involving podand b05 showed all seven oxygen atoms involved in

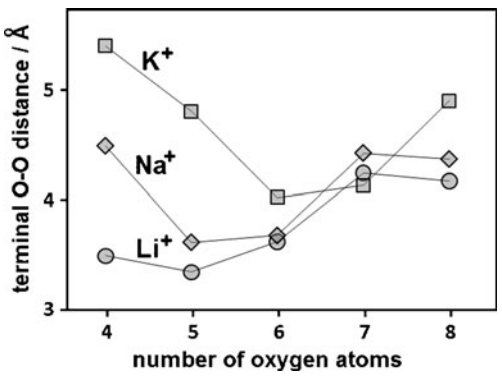


**Fig. 3** Plot of the distance between the two terminal oxygen atoms for each complex (○ $Li^+$, ◇ $Na^+$, □ $K^+$), as a function of the number of oxygen atoms present

**Table 1** Enthalpy (ΔH), entropy (as T·ΔS) and free energy (ΔG) differences (in kcal $mol^{-1}$) for the process defined by Eq. 2

| | $Li^+$ | | | $Na^+$ | | | $K^+$ | | |
|---|---|---|---|---|---|---|---|---|---|
| | ΔH | T·ΔS | ΔG | ΔH | T·ΔS | ΔG | ΔH | T·ΔS | ΔG |
| b02 | 10.21 | -1.79 | 12.00 | 4.58 | -2.37 | 6.95 | 2.65 | -2.46 | 5.11 |
| b03 | 13.05 | -3.53 | 16.58 | 7.34 | -3.50 | 10.84 | 4.13 | -1.56 | 5.69 |
| b04 | 14.51 | -2.56 | 17.07 | 8.12 | -1.76 | 9.88 | 4.84 | -1.14 | 5.98 |
| b05 | 19.56 | -4.30 | 23.86 | 11.06 | -3.44 | 14.50 | 6.17 | -3.00 | 9.17 |
| b06 | 14.87 | -4.28 | 19.15 | 12.06 | -3.56 | 15.62 | 6.53 | -1.68 | 8.21 |
| b11 | 8.83 | -2.83 | 11.66 | 3.58 | -3.23 | 6.81 | 2.88 | -0.69 | 3.57 |
| b22 | 13.65 | -5.77 | 19.42 | 9.37 | -4.48 | 13.85 | 3.65 | -3.93 | 7.58 |
| b33 | 13.13 | -6.35 | 19.48 | 12.20 | -3.89 | 16.09 | 8.78 | -2.93 | 11.71 |
| b44 | 17.95 | -5.78 | 23.73 | 10.72 | -2.98 | 13.70 | 6.92 | -1.75 | 8.67 |

strong interactions, surrounding the cation in a helical-type geometry, at a mean distance of 2.844 (±0.044) Å and with a mean dihedral angle value of 62.5° (±1.8°). The octadentate podands b33 and b06 also use all oxygen atoms in strong interactions with the cation at distances of 2.891 (±0.060) Å and 2.884 (±0.039) Å, respectively, involving the cation in an almost spherical way. The corresponding mean dihedral angle values are 62.6° (±3.4°) and 64.2° (±1.5°). The potentially decadentate podand b44 forms a heptadentate complex with a mean distance of 2.816 (±0.046) Å, leaving three oxygen atoms in one of the podand arms free, at 4.822 Å, 6.349 Å and 6.520 Å of the $K^+$ cation and a mean dihedral angle value of 62.8° (±1.5°).

The $K^+$–O mean distance is also found to increase with the coordination number of the complex: 2.716 (±0.003) Å for the tetracoordinated cation (considering complexes involving podands b02 and b11), 2.756 Å for the pentacoordinated cation (considering the complex involving podands b03), 2.814 (±0.037) Å for the hexacoordinated cation (considering complexes involving podands b04 and b22), 2.830 (±0.019) Å for the heptacoordinated cation (considering complexes involving podands b05 and b44) and 2.887

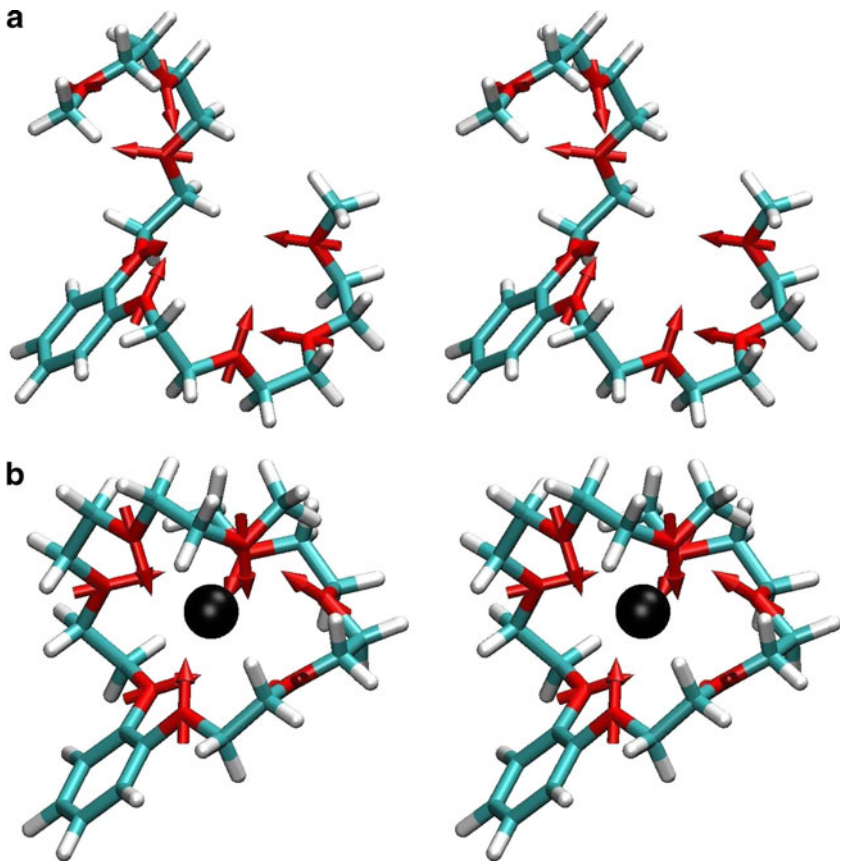


**Fig. 4** Stereo-view of the optimized structures for podand b33 in the free form, *L*, (**a**) and in complex (with $K^+$ as the *central black sphere*) form, *L**, (**b**), featuring the OCO dipoles as *red arrows*

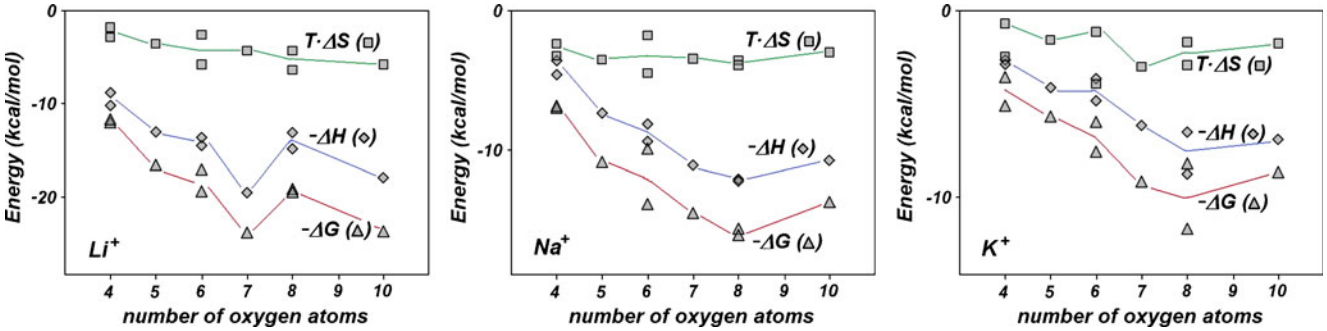


**Fig. 5** Plots of free energy (−ΔG, -△-), enthalpy (−ΔH, -◇-) and entropy (as T·ΔS, -□-) for the process defined by Eq. 2 for each cation, as a function of the number of oxygen atoms present in the podand

(±0.005) Å for the octacoordinated cation (considering complexes involving podands b06 and b33). As with the other cations, the OC–CO dihedral angle also increases from 60.5° (±0.1°) in tetracoordination to 61.9° in pentacoordination, to 62.3° (±1.1°) in hexacoordination, to 62.6° (±0.15°) in heptacoordination and to 63.4° (±1.1°) in octacoordination.

It is noteworthy that the distance between the terminal oxygen atoms for the optimized structures of the complexes (Fig. 3) is smallest for the podands with 4 or 5 oxygen atoms when involving $Li^+$, for the podands with 5 or 6 oxygen atoms when involving $Na^+$, and for the podands with 6 or 7 oxygen atoms when involving $K^+$.

## Structural adaptation of the podands during complexation

Optimization of the free podands (*L*) in vacuum followed by hessian calculations allowed the estimation of (zero point corrected) thermodynamical parameters [enthalpy (ΔH), entropy (as T·ΔS) and free energy (ΔG)]. After removal of the cations from the previously optimized complex structures, single point hessian calculations on the resulting podand structures (*L**) allowed estimation of the above mentioned thermodynamical parameters corresponding to the podands in the conformations adopted in their complexes. The calculated variations in ΔH, T·ΔS and ΔG corresponding to the conversion of *L* into *L** defined by equation

$$L \rightleftharpoons L^* \qquad (2)$$

are presented in Table 1.

The conversion of all podands from their free structures into the structures they present in the complexes is invariably unfavorable from an enthalpic point of view. This was expected due to the strains induced by the adoption of a complexation prone structure which also implies the enthalpically unfavorable redirection of C–O–C dipoles [56, 57] towards the center of the pseudo-cavity in order to accommodate the central cation (see the illustrative example of b33 in Fig. 4), and also the enthalpically unfavorable strains due to the OC–CO dihedral angle decrease [58] verified when both oxygen atoms are involved in coordination.

All the conversions of *L* into *L** are also entropically unfavorable as the adoption of a complexation-prone structure implies a lowering of the podand entropy. The destabilization induced by this factor is rather low and constant when compared with the unfavorable enthalpic factor, as may be seen in Fig. 5. As a result, all conversions present unfavorable free energies. During complexation, these destabilizations are more than compensated (at least enthalpically) by the formation of strong interactions between the podand oxygen atoms and the central cation, as will be shown below.

From analysis of the graphs presented in Fig. 5, two points are noteworthy: (1) on going from the $Li^+$ complex to the $K^+$ complex forms, the process $L \rightleftharpoons L^*$ becomes gradually less unfavorable; and (2) a dependence of the ΔH and ΔG values (the T·ΔS values are almost constant throughout) on the number of oxygen atoms present is clear: before a specific number of strongly interacting oxygen atoms is reached for each cation (six for $Li^+$, seven for $Na^+$ and eight for $K^+$), a strong increase in enthalpic destabilization is visible when the number of oxygen atoms present in the podands increases but, after that number is

**Table 2** Counterpoise corrected cation–podand interaction energies (in kcal $mol^{-1}$)

| | $Li^+$ | $Na^+$ | $K^+$ |
|---|---|---|---|
| b02 | -103.01 | -72.46 | -52.85 |
| b03 | -115.75 | -85.31 | -63.20 |
| b04 | -120.73 | -95.93 | -73.08 |
| b05 | -126.42 | -101.48 | -79.64 |
| b06 | -126.70 | -107.02 | -86.23 |
| b11 | -102.25 | -72.79 | -52.99 |
| b22 | -120.21 | -95.89 | -71.22 |
| b33 | -121.58 | -103.58 | -85.73 |

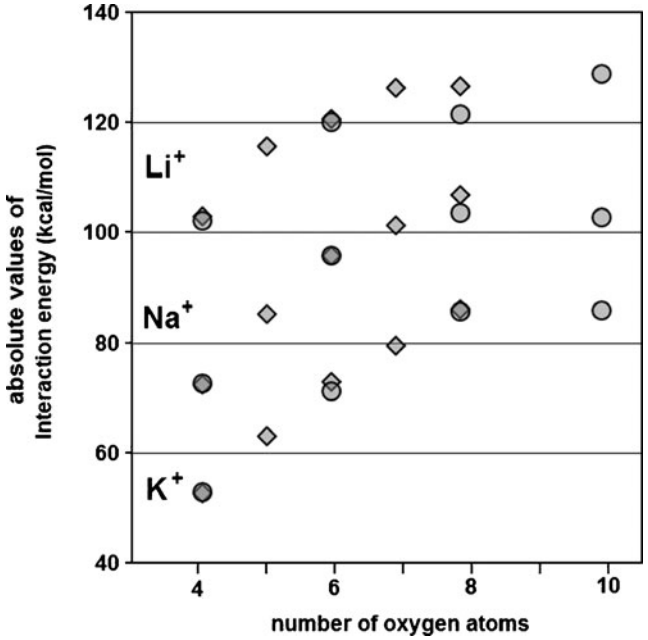


**Fig. 6** Absolute values of the counterpoise corrected cation/podand interaction energies found for the complexes of $Li^+$, $Na^+$ and $K^+$, and the symmetrical (o) and asymmetrical (◇) podands, as a function of the number of oxygen atoms present

reached, the destabilization rate is much lower, pointing to the less important role played by the "extra" oxygen atoms present in the podands during complexation.

## Cation/podand interaction energies

The counterpoise corrected cation/podand interaction energy values found for the complexes of $Li^+$, $Na^+$ and $K^+$ with the symmetrical (b11 to b44) and asymmetrical (b02 to b06) podands are presented in Table 2 (and Fig. 6). Notably, different podand symmetries do not seem to induce any significant difference in the interaction energies as the values found for complexes involving podands with the same number of oxygen atoms but with different symmetry are very close to each other.

The $Li^+$ complexes show the strongest interaction energies found among the complexes studied in the present work. There is an increase (in absolute terms) of 8.1 (± 3.9) kcal $mol^{-1}$ per oxygen atom until the podand oxygen number is about six. For complexes involving podands with six or more oxygen atoms, the interaction energy shows a much less pronounced increase. These results are consistent with the saturation of the $Li^+$ coordination shell by six oxygen atoms already hinted at above. As for the $Na^+$ complexes, there is also an initial increase (in absolute terms) in the interaction energy of 9.2 (± 3.2) kcal $mol^{-1}$ per oxygen atom, as the number of podand oxygen atoms increases up to ca. 7. After that number is reached, the interaction energy stabilizes, pointing to saturation of the $Na^+$ coordination shell by the seven oxygen atoms as already pointed out above. In the case of $K^+$ complexes, the increase (in absolute terms) of 8.3 (± 1.7) kcal $mol^{-1}$ per oxygen atom in the interaction energy is extended to all complexes involving podands with up to eight oxygen atoms. All the calculated increases in interaction energy per oxygen atom are statistically equal (at a significance level higher that 99%), and their mean value is 8.5 kcal $mol^{-1}$. The complex involving the podand b44, with ten potential donor oxygen atoms, shows an interaction energy almost equal to that found for the complex involving the podands b33 and b06, both of which have eight potential donor oxygen atoms, indicating that the $K^+$ coordination sphere is saturated when eight oxygen atoms are involved in strong interactions, as already implied in preceding sections.

## Thermodynamics of cation complexation

In this section, we report and discuss the thermodynamical data calculated for the complexation steps involving the cations $Li^+$, $Na^+$ and $K^+$ and each of the podands (b02–b06 and b11–b44), in three different media (vacuum, dichloromethane and water).

**Table 3** Enthalpy (ΔH), entropy (as T·ΔS) and free energy (ΔG) differences (in kcal $mol^{-1}$) for the process defined by Eq. 3

| | $Li^+$ | | | $Na^+$ | | | $K^+$ | | |
|---|---|---|---|---|---|---|---|---|---|
| | ΔH | T·ΔS | ΔG | ΔH | T·ΔS | ΔG | ΔH | T·ΔS | ΔG |
| b02 | -94.90 | -10.79 | -84.11 | -69.56 | -10.29 | -59.27 | -49.46 | -9.41 | -40.05 |
| b03 | -105.38 | -13.28 | -92.10 | -79.94 | -11.80 | -68.14 | -58.91 | -10.80 | -48.11 |
| b04 | -108.23 | -11.00 | -97.23 | -90.15 | -10.97 | -79.18 | -67.42 | -8.72 | -58.70 |
| b05 | -109.06 | -12.61 | -96.45 | -92.29 | -11.95 | -80.34 | -72.85 | -11.31 | -61.54 |
| b06 | -114.20 | -14.08 | -100.12 | -96.50 | -12.60 | -83.90 | -79.78 | -12.08 | -67.70 |
| b11 | -95.24 | -9.90 | -85.34 | -70.46 | -9.76 | -60.70 | -49.43 | -8.94 | -40.49 |
| b22 | -108.46 | -12.87 | -95.59 | -88.49 | -12.81 | -75.68 | -66.84 | -11.75 | -55.09 |
| b33 | -109.90 | -15.06 | -94.84 | -93.66 | -14.53 | -79.13 | -76.98 | -13.74 | -63.24 |
| b44 | -111.88 | -11.75 | -100.13 | -93.46 | -10.75 | -82.71 | -78.86 | -11.51 | -67.35 |

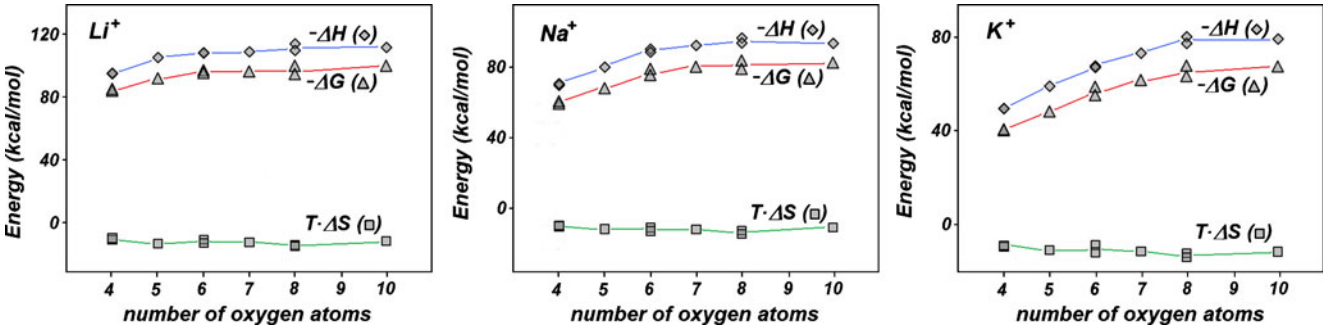


**Fig. 7** Plots of free energy (−ΔG, -△-), enthalpy (−ΔH, -◇-) and entropy (as T·ΔS, -□-) for the process defined by Eq. 3 for each cation, as a function of the number of oxygen atoms present in the podand

*In vacuum*

The complexation of $Li^+$, $Na^+$ and $K^+$ cations by podands in vacuum may be represented by the equation

$$M^+ + L \rightleftharpoons ML^+ \tag{3}$$

This is the simplest system to study as all intervening species are free (not solvated). Analysis of the pertinent thermodynamic parameters (Table 3 and Fig. 7) indicates that the complexation process is highly favorable, and mostly enthalpically driven as the entropic contribution is unfavorable to complexation but considerably lower and almost constant in value.

The initial favorable variation of enthalpy and free energy with the increase in the number of potentially donor oxygen atoms stops when a specific number of oxygen atoms is reached: six for $Li^+$, seven for $Na^+$ and eight for $K^+$.

*In dichloromethane*

To study the effect of the solvent on the complexation we used a simple model in which we considered the reaction of the tetra-solvated cations with the free podands, originating from the corresponding complexes and four solvent molecules. The corresponding complexation process may be represented by the equation

$$\left[M(CH_2Cl_2)_4\right]^+ + L \rightleftharpoons [ML]^+ + 4CH_2Cl_2 \tag{4}$$

Analysis of the thermodynamic parameters (Table 4 and Fig. 8) indicates that the complexation process is in all cases favorable (more so for $Li^+$ than for $Na^+$, and more so for $Na^+$ than for $K^+$) and mostly enthalpically driven. The entropic contribution to complexation is almost constant for each cation and seems to be almost independent of the number of oxygen atoms present in the podand. Comparatively, within cations, there is a small decrease in entropic stabilization on going from $Li^+$ to $K^+$.

As seen above, for the complexation in vacuum, the initial favorable enthalpy and free energy variations with the number of potentially donor oxygen atoms stop when specific numbers of podand oxygen atoms are reached for each cation. By considering the dichloromethane solvated cation, there is a considerable lowering of the favorable complexation enthalpy and free energy values and an increase in complexation entropy relative to the process in vacuum.

**Table 4** Enthalpy (ΔH), entropy (as T·ΔS) and free energy (ΔG) differences (in kcal $mol^{-1}$) for the process defined by Eq. 4

| | $Li^+$ | | | $Na^+$ | | | $K^+$ | | |
|---|---|---|---|---|---|---|---|---|---|
| | ΔH | T·ΔS | ΔG | ΔH | T·ΔS | ΔG | ΔH | T·ΔS | ΔG |
| b02 | -35.62 | 23.53 | -59.16 | -21.86 | 22.07 | -43.93 | -14.49 | 17.14 | -31.63 |
| b03 | -46.10 | 21.05 | -67.15 | -32.24 | 20.56 | -52.80 | -23.95 | 15.74 | -39.68 |
| b04 | -48.96 | 23.33 | -72.28 | -42.45 | 21.38 | -63.83 | -32.45 | 17.82 | -50.28 |
| b05 | -49.79 | 21.72 | -71.50 | -44.59 | 20.40 | -64.99 | -37.88 | 15.24 | -53.12 |
| b06 | -54.93 | 20.24 | -75.17 | -48.79 | 19.76 | -68.56 | -44.82 | 14.45 | -59.27 |
| b11 | -35.97 | 24.43 | -60.39 | -22.76 | 22.59 | -45.35 | -14.47 | 17.60 | -32.07 |
| b22 | -49.18 | 21.46 | -70.64 | -40.79 | 19.55 | -60.34 | -31.88 | 14.79 | -46.67 |
| b33 | -50.63 | 19.26 | -69.89 | -45.96 | 17.82 | -63.78 | -42.02 | 12.80 | -54.81 |
| b44 | -52.60 | 22.58 | -75.18 | -45.76 | 21.61 | -67.37 | -43.89 | 15.03 | -58.93 |

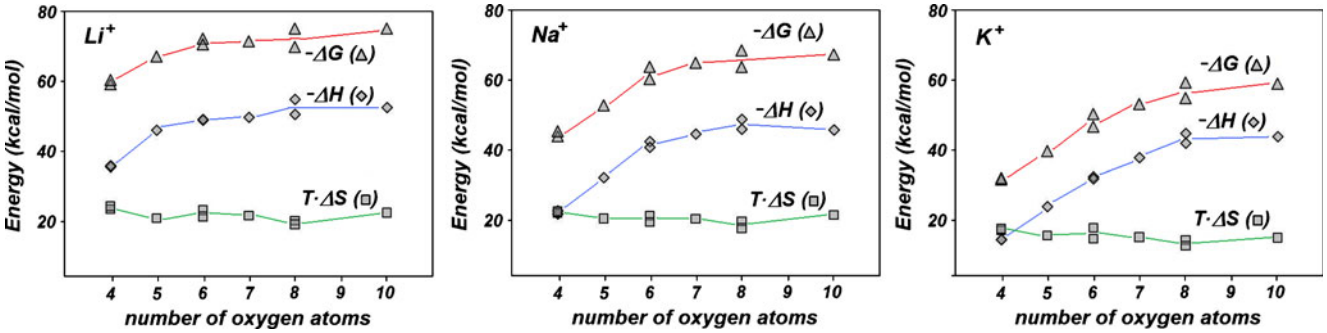


**Fig. 8** Plots of free energy (−ΔG, -△-), enthalpy (−ΔH, -◇-) and entropy (T·ΔS, -□-) for the process defined by Eq. 4 for each cation, as a function of the number of oxygen atoms present in the podand

*In water*

We applied the model described above to cation complexation in water. The complexation process may be described by the equation

$$\left[M(H_2O)_4\right]^+ + L \rightleftharpoons [ML]^+ + 4H_2O \qquad (5)$$

The corresponding thermodynamic parameters (Table 5 and Fig. 9) indicate that the complexation process is energetically favorable and mostly entropically driven for the $Li^+$ cation, and both entropically and enthapically driven for the $Na^+$ and $K^+$ cations. The entropic contribution to complexation is always favorable. The enthalpic contribution is mostly favorable, except for the complexation involving the potentially tetradentate podands b02 and b11. Again, as previously seen in vacuum and in dichloromethane, the enthalpy and the free energy values increase with the increase in the number of potentially donor oxygen atoms until critical coordination numbers are reached.

Our results point to a strong lowering of the favorable complexation enthalpy and free energy values and a gradual increase in the favorable complexation entropy for the complexation process in water when compared to the equivalent processes in vacuum and in dichloromethane.

Podand extraction efficiency

In a typical alkali cation extraction experiment the cations are present in the aqueous phase and the extracting agents are present in the organic phase. Molecular dynamics results [58] suggest that the cation complexation step takes place in the organic phase (dichloromethane in the present work). We considered the transference of the cation from the aqueous phase to the organic phase as defined by Eq. 6

$$\left[M(H_2O)_4\right]^+ + 4\,CH_2Cl_2 \rightleftharpoons \left[M(CH_2Cl_2)_4\right]^+ + 4\,H_2O \qquad (6)$$

followed by the cation complexation as defined by Eq. 4 to model the extraction process. In fact, this process may be globally translated by Eq. 5.

Estimation of the corresponding values of $K_{extr}$ is straightforward by substitution of the values of $\Delta G_{extr}$ in

**Table 5** Enthalpy (ΔH), entropy (as T·ΔS) and free energy (ΔG) differences (in kcal $mol^{-1}$) for the process defined by Eq. 5

| | $Li^+$ | | | $Na^+$ | | | $K^+$ | | |
|---|---|---|---|---|---|---|---|---|---|
| | ΔH | T·ΔS | ΔG | ΔH | T·ΔS | ΔG | ΔH | T·ΔS | ΔG |
| b02 | 8.85 | 20.29 | -11.44 | 8.66 | 16.49 | -7.83 | 8.29 | 16.30 | -8.01 |
| b03 | -1.63 | 17.80 | -19.43 | -1.71 | 14.98 | -16.70 | -1.17 | 14.90 | -16.07 |
| b04 | -4.48 | 20.08 | -24.56 | -11.93 | 15.81 | -27.73 | -9.67 | 16.99 | -26.66 |
| b05 | -5.31 | 18.47 | -23.78 | -14.06 | 14.83 | -28.89 | -15.10 | 14.40 | -29.50 |
| b06 | -10.45 | 17.00 | -27.45 | -18.27 | 14.19 | -32.46 | -22.04 | 13.62 | -35.65 |
| b11 | 8.51 | 21.18 | -12.67 | 7.76 | 17.02 | -9.25 | 8.32 | 16.76 | -8.45 |
| b22 | -4.71 | 18.21 | -22.92 | -10.27 | 13.97 | -24.24 | -9.10 | 13.96 | -23.05 |
| b33 | -6.16 | 16.02 | -22.17 | -15.43 | 12.25 | -27.68 | -19.23 | 11.96 | -31.20 |
| b44 | -8.13 | 19.33 | -27.46 | -15.23 | 16.03 | -31.27 | -21.11 | 14.20 | -35.31 |

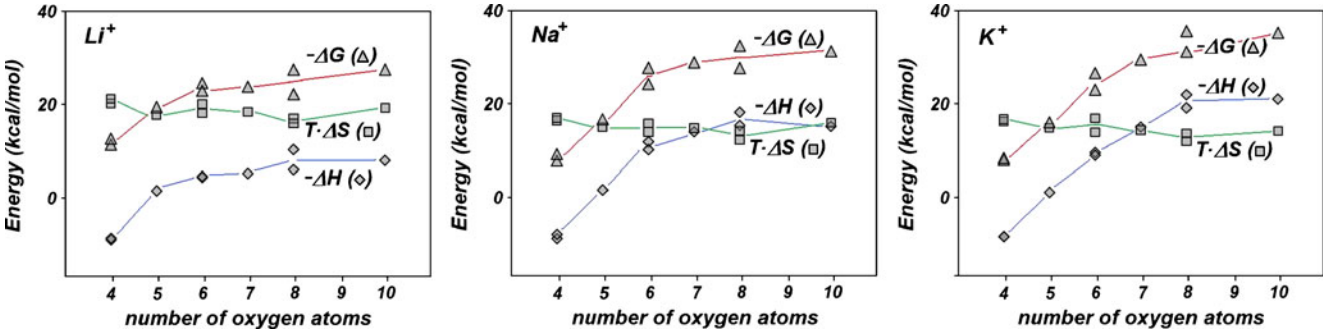


**Fig. 9** Plots of free energy (−ΔG, -△-), enthalpy (−ΔH, -◇-) and entropy (−T·ΔS, -□-) for the process defined by Eq. 5 for each cation, as a function of the number of oxygen atoms present in the podand

expression $K_{extr}=e^{-\Delta Gextr/RT}$. The results are presented in Table 6 as the corresponding decimal logarithms, along with the previously determined [59] experimental values.

Analysis of the data presented in Table 6 reveals clearly that the calculated values are considerably higher than the experimental values. This has also been observed in other studies on alkali cation complexation by coronands [41–44, 60]. Some of the reasons proposed to explain this discrepancy are: (1) neglect of the free podand and of the complex solvation; (2) the overlooking of higher hydration numbers for the cations; (3) the disregard of changes in solvent–solvent and solute–solvent intermolecular interactions during complexation reactions; (4) the fact that the influence of the anion (usually picrate), even as a separated ion pair, is not considered; and (5) the fact that only few (one in our case) conformations for each free ionophore, each complex and each solvated cation were considered, i.e., the assumption that the conformations considered are representative of the most probable ones in solution.

In our work, however, the trends found are qualitatively correct and, by applying a least squares fit of the calculated $\log(K)_{extr}$ values to the corresponding experimental values [59], we obtained scale factors for each ion (0.1597 for $Li^+$, 0.1339 for $Na^+$ and 0.1550 for $K^+$). The application of these correcting factors to the calculated log ($K_{extr}$) values result in the adjusted constant values present in Table 7, which agree reasonably well with experimental values (Fig. 10). Furthermore, the closeness of the scale factors to each other hints at a common reason for the energetic difference between the raw calculated values and the experimental ones.

Operatively, a comparison of the selectivities may be achieved when one considers the quotient of the $\log(K_{extr})$ values for two cations and the same podand. Table 7 lists the abovementioned quotients for the extraction of $Li^+$ and $Na^+$ relative to $K^+$, for the experimental values for $\log(K_{extr})$ [58] and for the corresponding values calculated in the present paper. From the graphical representations of these quotients presented in Fig. 11, one is able to identify effective correlations for the $Li^+$ values (slope=1.13 and $r^2$=0.94) and for the $Na^+$ values (slope=0.74 and $r^2$=0.60). Although a poorer correlation for the $Na^+$ cation is found both slopes approach the ideal value of 1, thus supporting our approach.

**Table 6** Experimental (*Exp.*), calculated (*Calc.*) and adjusted (*Adj.*) $\log(K_{extr})$ values for the extraction process

| | $Li^+$ | | | $Na^+$ | | | $K^+$ | | |
|---|---|---|---|---|---|---|---|---|---|
| | Exp. | Calc. | Adj. | Exp. | Calc. | Adj. | Exp. | Calc. | Adj. |
| b02 | 2.46 | 8.39 | 1.34 | 1.61 | 5.74 | 0.77 | 1.78 | 5.88 | 0.91 |
| b03 | 2.53 | 14.25 | 2.28 | 2.10 | 12.25 | 1.64 | 2.16 | 11.78 | 1.83 |
| b04 | 2.67 | 18.02 | 2.88 | 2.51 | 20.34 | 2.72 | 2.68 | 19.55 | 3.03 |
| b05 | 2.75 | 17.44 | 2.79 | 2.72 | 21.19 | 2.84 | 3.31 | 21.63 | 3.35 |
| b06 | 2.67 | 20.14 | 3.22 | 2.79 | 23.81 | 3.19 | 3.52 | 26.15 | 4.05 |
| b11 | 2.55 | 9.29 | 1.48 | 1.77 | 6.79 | 0.91 | 1.94 | 6.20 | 0.96 |
| b22 | 2.56 | 16.81 | 2.68 | 2.38 | 17.78 | 2.38 | 2.91 | 16.91 | 2.62 |
| b33 | 2.70 | 16.26 | 2.60 | 2.91 | 20.30 | 2.72 | 3.71 | 22.88 | 3.55 |
| b44 | 2.86 | 20.14 | 3.22 | 2.89 | 22.93 | 3.07 | 3.95 | 25.90 | 4.01 |

## Conclusions

Analysis of the optimized structures of the complexes reveals that the increase in the coordination number brings about an increase in the mean cation–oxygen distances, and in the OC–CO dihedral angles, apparently to better accommodate the cation on going from $Li^+$ to $Na^+$, to $K^+$. Also from the optimized structural results, the distance to both terminal oxygen atoms is smallest in $Li^+$ complexes, for podands with 4 to 5 oxygen atoms; in $Na^+$ complexes, for podands with 5 to 6 oxygen atoms and in $K^+$ complexes, for podands with 6 to 7 oxygen atoms. These results compare reasonably well with those reported for the coronands 12-crown-4 and 15-crown-5, 18-crown-6 and 21-crown-7 that form the most stable complexes with these cations in vacuo, as determined experimentally.

The thermodynamic properties calculated for the processes of adaptation undergone by the podands during complexation show that they are not enthalpically, or entropically, favorable.

The calculated BSSE-corrected cation-podand interaction energies were seen to vary with the number of oxygen atoms present in the podands, increasing up to a value that depends on the cation (six for $Li^+$, seven for $Na^+$ and eight for $K^+$). From the interaction energy point of view, podand symmetry seems to play a minor role in the complexation process.

The thermodynamic values calculated for the complexation processes suggest that, on going from vacuum to dichloromethane, and then to water, the absolute values of the complexation enthalpies decrease significantly (disfavoring the complexation), the absolute values of the complexation entropies increase somewhat (favoring the complexation) and, as a result, the absolute values of the complexation free energies decrease considerably (disfavoring the complexation). This result is in accord with the frequent observation that alkali cation complexation by polyether-type molecules is less favored in water than in organic solvents (such as chloroform and dichloromethane), and more so than in vacuum.

**Table 7** Values of the quotients of the experimental and calculated $\log(K_{extr})$ constants for $Li^+$ and $Na^+$ relative to the $K^+$ values

| | $(Li^+/K^+)_{Exp.}$ | $(Li^+/K^+)_{Calc.}$ | $(Na^+/K^+)_{Exp.}$ | $(Na^+/K^+)_{Calc.}$ |
|---|---|---|---|---|
| b02 | 1.38 | 1.43 | 0.90 | 0.98 |
| b03 | 1.17 | 1.21 | 0.97 | 1.04 |
| b04 | 1.00 | 0.92 | 0.93 | 1.04 |
| b05 | 0.83 | 0.81 | 0.82 | 0.98 |
| b06 | 0.76 | 0.77 | 0.79 | 0.91 |
| b11 | 1.32 | 1.50 | 0.91 | 1.10 |
| b22 | 0.88 | 0.99 | 0.82 | 1.05 |
| b33 | 0.73 | 0.71 | 0.78 | 0.89 |
| b44 | 0.72 | 0.78 | 0.73 | 0.89 |

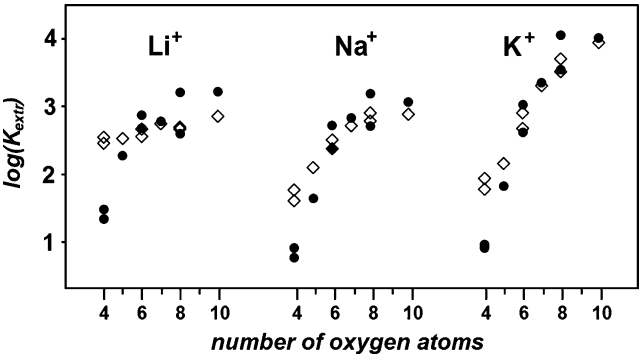


**Fig. 10** Plots of the experimental (●) and calculated (◇) $\log(K_{extr})$ values

The podand extraction efficiency was assessed by means of a simple model based on the consideration that the complexation process happens mainly in the dichloromethane phase, and is preceded by the exchange of four waters of hydration for four dichloromethane molecules. The calculated thermodynamic data allowed the estimation of extraction constants that follow the experimental trends qualitatively but are much higher in value than the experimental values. By a least squares method, it was possible to find scale factors (for each cation) that, when applied to the decimal logarithms of the calculated extraction constants, result in a reasonable agreement with experimental values. The similarity of the scale factors suggests a common reason for the overestimation of the predicted values.

Experimental and calculated podand extraction selectivities [for each podand, taken as the quotient of the $\log(K_{extr})$ for $Li^+$ or $Na^+$ and the $\log(K_{extr})$ for $K^+$] are also in good agreement, supporting our simple model and analysis.

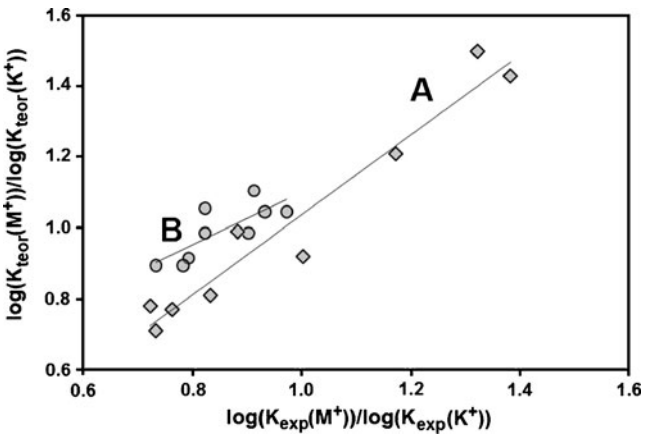


**Fig. 11** Plots of the quotients of the experimental and calculated log ($K_{extr}$) values for $Li^+$ (**A**) and $Na^+$ (**B**) relative to $K^+$. The *straight lines* represent the corresponding linear correlations

## References


1. Pedersen CJ (1967) Cyclic polyethers and their complexes with metal salts. J Am Chem Soc 89:7017–7036. doi:10.1021/ja01002a035
2. Pedersen CJ (1988) The discovery of crown ethers (Nobel lecture). Angew Chem Int Ed Engl 27:1021–1027. doi:10.1002/anie.198810211
3. Cram D (1988) The design of molecular hosts, guests, and their complexes (Nobel lecture). Angew Chem Int Ed Engl 27:1009–1020. doi:10.1002/anie.198810093
4. Lehn JM (1988) Supramolecular chemistry—scope and perspectives: molecules, supermolecules, molecular devices (Nobel lecture). Angew Chem Int Ed Engl 27:89–112. doi:10.1002/anie.198800891
5. Bovill MJ, Chadwick DJ, Sutherland IO (1980) Molecular mechanics calculations for ethers. The conformations of some crown ethers and the structure of the complex of 18-crown-6 with benzylammonium thiocyanate. J Chem Soc Perkin Trans 2 1529–1543. doi:10.1039/P29800001529
6. Wipff G, Weiner P, Kollman PA (1982) A molecular-mechanics study of 18-crown-6 and its alkali complexes: an analysis of structural flexibility, ligand specificity, and the macrocyclic effect. J Am Chem Soc 104:3249–3258. doi:10.1021/ja00376a001
7. Grootenhuis PDJ, Kollman PA (1989) Molecular mechanics and dynamics studies of crown ether - cation interactions: free energy calculations on the cation selectivity of dibenzo-18-crown-6 and dibenzo-30-crown-10. J Am Chem Soc 111:2152–2158. doi:10.1021/ja00188a032
8. Mazor MH, McCammon JA, Lybrand TP (1990) Molecular recognition in nonaqueous solvent. 2. Structural and thermodynamic analysis of cationic selectivity of 18-crown-6 in methanol. J Am Chem Soc 112:4411–4419. doi:10.1021/ja00167a044
9. Wang J, Kollman PA (1998) Alkali Cation Extraction by 18-Crown-6 and Its Derivatives: A Free Energy Perturbation Study. J Am Chem Soc 120:11106–11114. doi:10.1021/ja980464l
10. Vayssière P, Wipff G (2003) Importance of counter-ions in alkali and alkaline-earth cation extraction by 18-crown-6: molecular dynamics studies at the water/sc-$CO_2$ interface. Phys Chem Chem Phys 5:2842–2850. doi:10.1039/B303058J
11. Troxler L, Wipff G (1994) Conformation and dynamics of 18-crown-6, cryptand 222, and their cation complexes in acetonitrile studied by molecular dynamics simulations. J Am Chem Soc 116:1468–1480. doi:10.1021/ja00083a036
12. Kollman PA, Wipff G, Singh UC (1985) Molecular mechanical studies of inclusion of alkali cations into anisole spherands. J Am Chem Soc 107:2212–2219. doi:10.1021/ja00294a002
13. Grootenhuis PDJ, Kollmann PA, Groenen LC, Reinhoudt DN, van Hummel GJ, Ugozzoli F, Andreetti GD (1990) Computational study of the structural, energetic, and acid-base properties of calix[4]arenes. J Am Chem Soc 112:4165–4176. doi:10.1021/ja00167a010
14. Miyamoto S, Kollman PA (1992) Molecular dynamics studies of calixspherand complexes with alkali metal cations: calculation of the absolute and relative free energies of binding of cations to a calixspherand. J Am Chem Soc 114:3668–3674. doi:10.1021/ja00036a015
15. Varnek A, Wipff GJ (1996) Theoretical calculations of extraction selectivity: alkali cation complexes of calix[4]-bis-crown6 in pure water, chloroform, and at a water/chloroform interface. J Comput Chem 17:1520–1513. doi:10.1002/(SICI)1096-987X(199610
16. Thuéry P, Nierlich M, Lamare V, Dozol J-F, Asfari Z, Vicens (1997) Potassium and sodium complexes of 1,3-calix[4]-*bis*-crown-6: crystal and molecular structures, $^1$H-NMR investigation and molecular dynamics simulation. J Supramol Chem 8:319–332. doi:10.1080/10610279708034951
17. Sieffert N, Wipff G (2006) Comparing an ionic liquid to a molecular solvent in the cesium cation extraction by a calixarene: a molecular dynamics study of the aqueous interfaces. J Phys Chem B 110:19497–19506. doi:10.1021/jp063045g
18. Auffinger P, Wipff G (1991) Hydration of the 222 cryptand and 222 cryptates studied by molecular dynamics simulations. J Am Chem Soc 113:5976–5988. doi:10.1021/ja00016a009
19. Auffinger P, Wipff G (1991) Molecular dynamics simulations on the protonated 222. $H^+$ and 222.2$H^+$ cryptands in water: Endo versus exo conformations. J Incl Phen Macrocyclic Chem 11:71-88. doi:10.1007/BF01073686
20. Jost P, Galand N, Schurhammer R, Wipff G (2002) The 222 cryptand and its cryptates at the water/"oil" interface: molecular dynamics investigations of concentrated solutions. Phys Chem Chem Phys 4:335–344. doi:10.1039/B104662B
21. Nazarenko AY, Baulin VE, Lamb JD, Volkova TA, Varnek AA, Wipff G (1999) Solvent extraction of metal picrates by phosphoryl-containing podands. Solvent Extr Ion Exch 17:495–523. doi:10.1080/07366299908934625
22. Solovév VP, Baulin VE, Strakhova NN, Kazachenko VP, Belski VK, Varnek AA, Volkova TA, Wipff G (1998) Complexation of phosphoryl-containing mono-, bi- and tri-podands with alkali cations in acetonitrile. Structure of the complexes and binding selectivity. J Chem Soc Perkin Trans 2 6:1489–1498. doi:10.1039/A708245B
23. Leska B, Pankiewicz R, Kira J, Schroeder G (2009) Potentiometric and AM1d studies of a new class of Tri-podands–silver(I) complexes. Supramol Chem 21:218–222. doi:10.1080/10610270802527028
24. Leska B, Pankiewicz R, Gierczyk B, Schroeder G (2008) Synthesis, structure and application of a new class of Tr-podands derived in phase-transfer catalysis. J Mol Catal A Chem 287:165–170. doi:10.1016/j.molcata.2008.03.011
25. Leska B, Pankiewicz R, Schroeder G, Gierczyk B, Maciejewski H, Marciniec M (2008) New type of repeated Si-C-podand catalysts for solid-liquid phase transfer reactions. Catal Commun 9:821–825. doi:10.1016/j.catcom.2007.09.012
26. Leska B, Pankiewicz R, Schroeder G, Maia A (2006) A new type of B-podand catalysts for solid-liquid phase transfer reactions. Tetrahedron Lett 47:5673–5676. doi:10.1016/j.tetlet.2006.06.016
27. Maia A, Landini D, Betti C, Leska B, Schroeder G (2005) Catalytic activity and anion activation in SN2 reactions promoted by complexes of silicon polypodands. Comparison with traditional polyethers. New J Chem 29:1195–1198. doi:10.1039/B504980F
28. Maia A, Landini D, Leska B, Schroeder G (2004) Silicon podands: a new class of efficient solid-liquid phase-transfer catalysts. Tetrahedron 60:10111–10115. doi:10.1016/j.tet.2004.06.049
29. Maia A, Landini D, Leska B, Schroeder G (2003) Silicon podands: powerful metal cation complexing agents and solid-liquid phase-transfer catalysts of new generation. Tetrahedron Lett 44:4149–4151. doi:10.1016/S0040-4039(03)00838-4
30. Turanov AN, Karandashev VK, Baulin VE, Yarkevich AN, Safronova ZV (2009) Extraction of lanthanides(III) from aqueous nitrate media with tetra-(*p*-tolyl)[(*o*-phenylene)oxymethylene] diphosphine dioxide. Solvent Extr Ion Exch 27:551–578. doi:10.1080/07366290903044683
31. Turanov AN, Karandashev VK, Baulin VE (2008) Effect of anions on the extraction of lanthanides(III) by N, N-dimethyl-N, N-diphenyl-3-hexapentanediamide. Solvent Extr Ion Exch 26:77–99. doi:10.1080/07366290801904871
32. Turanov AN, Karandashev VK, Baulin VE (2007) Extraction of lanthanides(III) from nitric acid solutions by selected polyfuctional monoacidic organophosphorus compounds. Solvent Extr Ion Exch 25:165–186. doi:10.1080/07366290601169410

33. Turanov AN, Karandashev VK, Baulin VE (2006) Extraction of rare-earth nitrates by phosphoryl podands. Russ J Inorg Chem 51:1829–1835. doi:10.1134/S0036023606110210
34. Nazarenko AY, Baulin VE, Lamb JD, Volkova TA, Varnek AA, Wipff G (1999) Solvent extraction of metal picrates by phosphoryl containing podands. Solvent Extr Ion Ex 17:495–523. doi:10.1080/07366299908934625
35. Turanov AN, Karandashev VK, Baulin VE (1999) Extraction of metal species from nitric acid solutions by phosphoryl-containing podands. Solvenet Extr Ion Exch 17:165–186. doi:10.1080/07366290601169410
36. Turanov AN, Karandashev VK, Baulin VE (1999) Extraction of rare-earth elements from nitric solutions by phosphoryl-containing podands. Solvent Extr Ion Exch 17:1423–1444. doi:10.1080/07366299908934656
37. Varnek AA, Ten-Elshof JE, Glebov AS, Solov'ev VP, Baulin VE, Tsvetkov EN (1992) Complexation of lithium and sodium cations with b-phosphorylate ethers, modeling terminal groups of organophosphorus podands: an experimental and theoretical study. J Mol Struct 271:311–325. doi:10.1016/0022-2860(92)80136-6
38. Yamabe T, Hori K, Akagi K, Fukui K (1979) Stability of crown ether complexes: a mo theoretical study. Tetrahedron 35:1065–1072. doi:10.1016/S0040-4020(01)93724-X
39. Hori K, Yamada H, Yamabe T (1983) Theoretical study on the nature of the interaction between crown ethers and alkali cations: Relation of interaction energy and ion selectivity. Tetrahedron 39:67–73. doi:10.1016/S0040-4020(01)97631-8
40. Ha YL, Chakraborty AK (1992) Nature of the interactions of 18-crown-6 with ammonium cations: a computational study. J Phys Chem 96:6410–6419. doi:10.1021/j100194a057
41. Glendening ED, Feller D, Thompson MA (1994) An ab initio investigation of the structure and alkali metal cation selectivity of 18-crown-6. J Am Chem Soc 116:10657–10669. doi:10.1021/ja00102a035
42. Feller D (1997) Ab initio study of $M^+$:18-crown-6 microsolvation. J Phys Chem A 101:2723–2731. doi:10.1021/jp9700185
43. Feller D, Thompson MA, Kendall RA (1997) A theoretical case study of substituent effects and microsolvation on the binding specificity of crown ethers. J Phys Chem A 101:7292–7298. doi:10.1021/jp971509s
44. Hill SE, Feller D, Glendening ED (1998) Theoretical study of cation/ether complexes: alkali metal cations with 1,2-dimethoxyethane and 12-crown-4. J Phys Chem A 102:3813–3819. doi:10.1021/jp980522p
45. Ali SKM, Maity DK, De S, Shenoi MRK (2008) Ligands for selective metal ion extraction: a molecular modeling approach. Desalination 232:181–190. doi:10.1016/j.desal.2007.09.017
46. Diao K-S, Wang H-J, Qiu Z-M (2009) A DFT study on the selective extraction of metallic ions by 12-crown-4. J Solution Chem 38:713–724. doi:10.1007/s10953-009-9406-3
47. Hou H, Zeng X, Liu X (2009) DFT study of a series of crown-4 ethers and their selectivity trend for alkali metal cations: $Li^+$ and $Na^+$. J Mol Model 15:105–111. doi:10.1007/s00894-008-0379-8
48. De S, Boda A, Ali SM (2010) Preferential interaction of charged alkali metal ions (guest) within a narrow cavity of cyclic crown ethers (neutral host): a quantum chemical investigation. J Mol Struct THEOCHEM 941:90–101. doi:10.1016/j.theochem.2009.11.009
49. Becke AD (1993) Density–functional thermochemistry. III. The role of exact exchange. J Chem Phys 98:5648. doi:10.1063/1.464913
50. Lee C, Yang W, Parr RG (1988) Development of the Colle-Salvetti correlation-energy formula into a functional of the electron density. Phys Rev B 37:785–789. doi:10.1103/PhysRevB.37.785
51. Frisch MJ, Trucks GW, Schlegel HB, Scuseria GE, Robb MA, Cheeseman JR, Montgomery Jr JA, Vreven T, Kudin KN, Burant JC, Millam JM, Iyengar SS, Tomasi J, Barone V, Mennucci B, Cossi M, Scalmani G, Rega N, Petersson GA, Nakatsuji H, Hada M, Ehara M, Toyota K, Fukuda R, Hasegawa J, Ishida M, Nakajima T, Honda Y, Kitao O, Nakai H, Klene M, Li X, Knox JE, Hratchian HP, Cross JB, Adamo C, Jaramillo J, Gomperts R, Stratmann RE, Yazyev O, Austin AJ, Cammi R, Pomelli C, Ochterski JW, Ayala PY, Morokuma K, Voth GA, Salvador P, Dannenberg JJ, Zakrzewski VG, Dapprich S, Daniels AD, Strain MC, Farkas O, Malick DK, Rabuck AD, Raghavachari K, Foresman JB, Ortiz JV, Cui Q, Baboul AG, Clifford S, Cioslowski J, Stefanov BB, Liu G, Liashenko A, Piskorz P, Komaromi I, Martin RL, Fox DJ, Keith T, Al-Laham MA, Peng CY, Nanayakkara A, Challacombe M, Gill PMW, Johnson B, Chen W, Wong MW, Gonzalez C, Pople JA (2004) Gaussian 03, Revision C.02. Gaussian Inc, Wallingford CT
52. Ochterski JW (2000) Thermochemistry in Gaussian. http://www.gaussian.com/g_whitepap/thermo.htm. Accessed 26 November 2010
53. Glendening ED, Feller D (1995) Cation-water interactions: the $M^+(H_2O)_n$ clusters for alkali metals, M=Li, Na, K, Rb, and Cs J Phys Chem 99:3060–3067. doi:10.1021/j100010a015
54. Mitani M, Yoshioka Y (2009) A B3LYP study on counterpoise-corrected geometry optimizations for hydrated complexes of $[K(H_2O)_n]^+$ and $[Na(H_2O)_n]^+$. J Mol Struct THEOCHEM 915:160–169. doi:10.1016/j.theochem.2009.08.030
55. Boys SF, Bernardi F (1970) The calculation of small molecular interactions by the differences of separate total energies. Some procedures with reduced errors. Mol Phys 19:553–566. doi:10.1080/00268977000101561
56. Cui C, Cho SJ, Kim KS (1998) Cation affinities of [1(6)]Starand Model. Comparison with 12-crown-4: crucial role of dipolar moiety orientations. J Phys Chem A 102:1119-1123. doi:10.1021/jp972591u
57. Hay BP, Rustad JR (1994) Structural criteria for the rational design of selective ligands: extension of the MM3 force field to aliphatic ether complexes of the alkali and alkaline earth cations. J Am Chem Soc 116:6316–6326. doi:10.1021/ja00093a035
58. Valente M, Sousa SF, Magalhães AL, Freire C (2010) A comparative molecular dynamics study on the complexation of alkali metal cations by a poly-ethylene-glycol type podand in water and in dichloromethane. J Mol Struct THEOCHEM 946:77–82. doi:10.1016/j.theochem.2009.10.025
59. Valente M, Sousa SF, Magalhães AL, Freire C (2010) Crown-ether type podands as alkali metal cation extractants: influence of the number of oxygens in the chain. J Solut Chem 39:1230–1242. doi:10.1007/s10953-010-9579-9
60. Feller D, Aprà È, Nichols JA, Bernholdt DE (1996) The structure and binding energy of $K^+$–ether complexes: a comparison of MP2, RI–MP2, and density functional methods. J Chem Phys 105:1940–1950. doi:10.1063/1.472082